NJC

Accepted Manuscript

This is an *Accepted Manuscript*, which has been through the Royal Society of Chemistry peer review process and has been accepted for publication.

Accepted Manuscripts are published online shortly after acceptance, before technical editing, formatting and proof reading. Using this free service, authors can make their results available to the community, in citable form, before we publish the edited article. We will replace this *Accepted Manuscript* with the edited and formatted *Advance Article* as soon as it is available.

You can find more information about *Accepted Manuscripts* in the Information for Authors.

Please note that technical editing may introduce minor changes to the text and/or graphics, which may alter content. The journal's standard Terms & Conditions and the Ethical guidelines still apply. In no event shall the Royal Society of Chemistry be held responsible for any errors or omissions in this *Accepted Manuscript* or any consequences arising from the use of any information it contains.

ROYAL SOCIETY OF CHEMISTRY

www.rsc.org/njc

Halogen, Chalcogen and Pnictogen Interactions in $(XNO_2)_2$ Homodimers (X = F, Cl, Br, I)

Cristina Trujillo[a] · Goar Sánchez-Sanz[b*] · Ibon Alkorta[c] · José Elguero[c]

[a] *School of Chemistry, Trinity Biomedical Sciences Institute, Trinity College, Trinity College, 152-160 Pearse St., Dublin 2, Ireland*

[b] *School of Physics & Complex and Adaptive Systems Laboratory, University College Dublin, Belfield, Dublin 4, Ireland*

[c] *Instituto de Química Médica, CSIC, Juan de la Cierva, 3, E-28006 Madrid, Spain*

Keywords Halogen bond, chalcogen bond, pnictogen bond, non covalent interactions

Graphical Abstract

Abstract

A theoretical study of the XNO_2 homodimers (X = F, Cl, Br and I) has been carried out by means of the Møller-Plesset (MP2) methodology. Twenty-two different minimum structures have been found, involving pnictogen, chalcogen and halogen bonds. MP2 interaction energies range between –0.4 to –17.5 kJ·mol^{-1}. Atoms in Molecules (AIM) and Natural Bond Orbital (NBO) approaches have been used to analyse the nature of the interaction within both monomers, obtaining good correlations between Laplacian values and bond distances. NBO $E^{(2)}$ orbital interaction energies are found to be up to 39.0 kJ·mol^{-1}. Charge transfer between monomers are in agreement with those in AIM and NBO findings, showing the highest charge transferred in those asymmetric dimers which involve pure halogen bonds. Symmetry Adapted Perturbation Theory (SAPT-DFT) results show that the interactions are driven by the dispersion term, followed by the electrostatic one. The induction term present the lowest contribution with the exception of complexes **1** and **5** of the iodine derivative in which $E_i^{(2)}$ shows the maximum contribution to the total forces.

Introduction

Non-covalent interactions between molecules play an important role in supramolecular chemistry, molecular biology, and materials science.[1] Among the weak interactions, hydrogen bond (HB) is without any doubt the most important. In recent years, a variety of new groups that can be involved in this interaction have been described. In fact, IUPAC has issued a new definition of HB in order to

categorize new information.[2] These advances occurred concurrently with the discovery of new kinds of non-covalent interactions, such as halogen bonds,[3] hydride bonds,[4] tetrels[5-7] or chalcogen-chalcogen interactions.[8-11]

The term pnictogen or pnicogen interaction has been coined for those Lewis acid-Lewis base attractive contacts where the interacting moiety in the Lewis acid (electron acceptor) is a pnictogen atom (N, P and As).

The possibility that pnictogen atoms act as Lewis acids has been known for several decades.[12-15] However, it was not until 2011 when Scheiner *et al.*[16, 17] and Hey-Hawking[18] simultaneously opened up this area of research. This has attracted the attention of the scientific community to these interactions. Since then, a number of articles have been devoted to the study and characterization of these interactions.[16, 17, 19-31] Much work has been performed in the field of pnictogen interactions,[32-41] with special attention to the binding energies, structural parameters, NMR properties and coupling constants.

The electrostatic nature of the pnictogen interactions has been rationalized based on the σ hole concept proposed by Politzer and Murray.[42-44] The term σ hole refers to the electron-deficient outer lobe of a p orbital involved in forming a covalent bond, especially when one of the atoms is highly electronegative. In those cases, when a region of positive electrostatic potential is perpendicular to a portion of a molecular framework, it is named as π-hole. The interaction of the nitrogen atom of the nitryl groups with electron donors can be simultaneously classified as an orthogonal and pnictogen interaction.[45]

On the other hand, great interest has been shown in recent years towards the so-called reservoir compounds in the atmosphere and great effort has been devoted to understanding their molecular properties, isomerization processes and the role of the related formation reactions in stratospheric ozone depletion cycles.[46, 47] Nitryl halides, XNO_2, have been suggested to be examples of such reservoir species.[48, 49] The potential interactions of the nitryl halides with NH_3,[50] NCH and CNH[51] molecules as electron donors in the σ- and π-hole regions have been previously studied with XNO_2 and other nitryl derivatives.[52] Experimental evidences of pnicogen interactions involving nitryl moieties have been recently reported by Roy *et al.*[53] In the present work, we have focused our attention on the nature of the non-covalent interactions found between a nitryl halides homodimers. Thus, the chemical groups attached to the nitryl moiety have been expanded along the halogen series, with F, Cl, Br and I atoms.

Computational Details

All the geometries of the complexes formed by two XNO_2 (X = F, Cl, Br and I) monomers were fully optimized at second order Møller-Plesset perturbation theory (MP2) with the aug-cc-pVTZ

basis set.[54, 55]. For heavy atoms, I[56] the aug-cc-pVTZ-PP pseudopotential basis set was used. Harmonic vibrational frequencies were computed at the same level used in order to verify that the structures obtained correspond to local minima. Single point calculations over the MP2 optimized geometry have been carried out at the CCSD(T)[57]/aug-cc-pVTZ computational level to obtain more accurate interaction energies. The interaction energies, E_b, have been calculated as the difference of the total energy of the complex and the sum of the isolated monomers.They have been studied with and without corrections for the inherent basis set superposition error (BSSE) using the Boys-Bernardi[58, 59] counterpoise technique on the optimized geometry. Additionally, we have estimated the interaction energies at the basis set limit using the method of Helgaker et al.[60, 61] from the calculated interaction energies with the aug-cc-pVDZ and aug-cc-pVTZ basis sets. All the calculations have been carried out with the Gaussian09 program.[62]

The molecular electrostatic potential (MEP) of the isolated monomers have been calculated on the electron density isosurface of 0.001 au. This isosurface has been shown to resemble the van der Waals surface.[63] These calculations have been carried out with the facilities of the Gaussian-09 program and the numerical results depicted using the WFA program.[64] Regions with negative MEP values are susceptible to interact with electron deficient moieties, such as HB donors, while positive regions can interact with electron rich areas.

The bonding characteristics were analyzed by means of the atoms in molecules (AIM) theory.[65, 66] For this purpose we have located the most relevant bond critical points (BCP), and evaluated the electron density at each of them, with the facilities of AIMALL programs.[67] All the interactions were characterized by the formation of a BCP between the atoms involved that are connected by the corresponding bond paths.

The Natural Bond Orbital (NBO) method[68] has been employed to evaluate atomic charges using the NBO-3.1 program, included within the Gaussian-09 program, and to analyse charge-transfer interactions between occupied and empty orbitals.

The SAPT (Symmetry Adapted Perturbation Theory)[69] method allows for the decomposition of the interaction energy into different terms related to physically well-defined components, such as those arising from electrostatic, exchange, induction, and dispersion terms. The interaction energy can be expressed within the framework of the SAPT method as:

$$E_{int} = E_{el}^{(1)} + E_{exch}^{(1)} + E_i^{(2)} + E_D^{(2)} \qquad (1)$$

where $E_{el}^{(1)}$ is the electrostatic interaction energy of the monomers each one with its unperturbed electron distribution; $E_{exch}^{(1)}$ is the first-order exchange energy term; $E_i^{(2)}$ denotes the second-order induction energy arising from the interaction of permanent multipoles with induced multipole

moments and charge-transfer contributions, plus the change in the repulsion energy induced by the deformation of the electronic clouds of the monomers; $E_D^{(2)}$ is the second-order dispersion energy, which is related to the instantaneous multipole-induced multipole moment interactions plus the second-order correction for coupling between the exchange repulsion and the dispersion interactions.

The DFT-SAPT formulation has been used to investigate interaction energies. In this approach, the energies of interacting monomers are expressed in terms of orbital energies obtained from Kohn-Sham density functional theory.[70, 71] In addition to the terms listed in eq. 1, a Hartree-Fock correction term δ(HF), which takes into account higher-order induction and exchange corrections, has been included.[72] The DFT-SAPT calculations have been performed using the PBE0/aug-cc-pVTZ/aug-cc-pVTZ-PP computational method.[73] Asymptotic corrections for this functional have been considered using the experimental values of the ionization potentials for NO_2F,[74] and NO_2Cl.[75] In the remaining cases, the calculated values at the MP2/aug-cc-pVTZ computational values have been used. All these calculations have been carried out with the MOLPRO program.[76]

Results and Discussion

Monomers

We have previously reported the structural data of XNO_2 monomers with X = F, Cl, Br and I[50, 52] and shown that theoretical results are in good agreement with the experimental data found in literature. For comparison purposes the electronic characteristics of those monomers have been studied, especially their molecular electrostatic potential, MEP (Table 1). Maxima and minima values of the MEP on the electron density isosurface that resembles the van der Waals surface (vdW) identify those areas susceptible to nucleophilic (a' and b') and electrophilic (a, b, and c) attacks.

The representation of the MEP over the vdW surface in Figure 1 also shows the region associated with the halogen lone pairs, halogen σ-hole, and the maxima over the nitrogen atom, called π-hole.

As previously observed, the σ-hole (a') becomes deeper with the halogen size, while the opposite is true for the π-hole (b'). It is worth noting that nitryl fluoride does not have a σ-hole along the F-N axis, as was observed in previous studies.[50, 52] Regarding the minima values of the MEP on the vdW isosurface, those associated with the halogen lone pair decrease with the size of X

atom. Two different electron lone pairs belonging to the oxygen atoms were located, the one closest to the halogen bond (b) and the furthest respect to the X (c). In the case of FNO_2, minimum b was not found. Minima c also varies with the halogen atom considered, the larger the electronegativity, the less negative the MEP minimum value on c.

Table 1. Molecular electrostatic potential (a.u.) on the 0.001 a.u. electron density isosurface at MP2/aug-cc-pVTZ level. Maxima along the X-N axis (σ-hole, a') and over the nitrogen atom (b'), minimum corresponding to X lone pairs (a) and two minima belonged to O lone pairs, close to the X atom (b) and further (c).

	a'	b'	a	b	c
NO_2F	–0.0162	0.0590	–0.0229	–	0.0027
NO_2Cl	0.0247	0.0490	–0.0085	–0.0154	–0.0062
NO_2Br	0.0346	0.0454	–0.0062	–0.0110	–0.0092
NO_2I	0.0494	0.0287	–0.0025	–0.0134	–0.0154

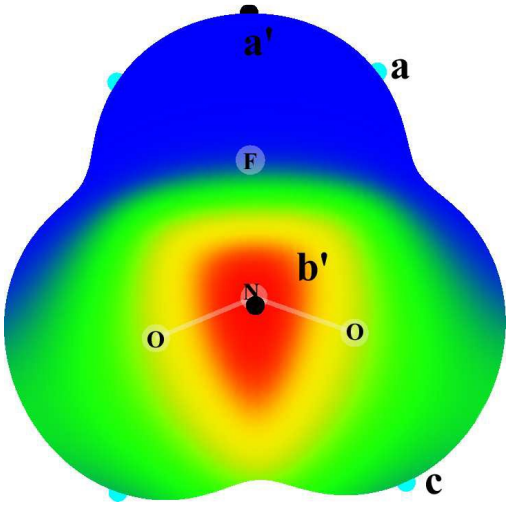

F

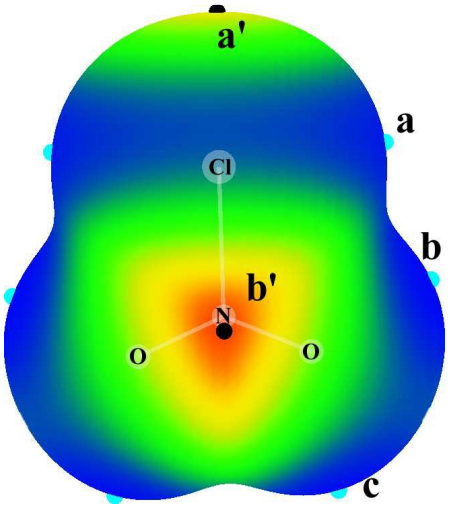

Cl

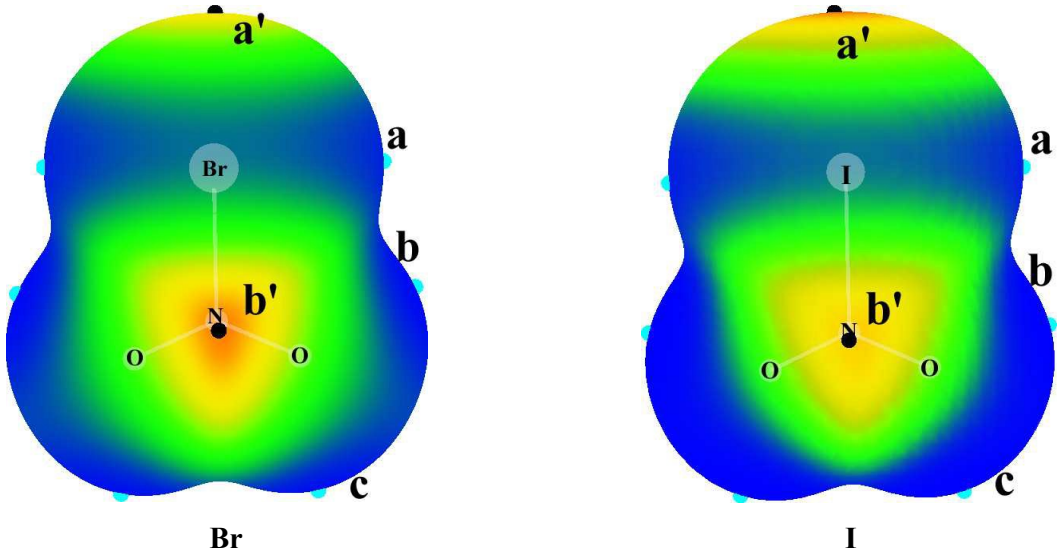

Figure 1. Molecular electrostatic potential on the 0.001 a.u. electron density isosurface of NO_2X (X = F, Cl, Br, and I) monomers. MEP values colour scheme: Red > 0.045 > Yellow > 0.019 > Green > 0.00 Blue < 0.00. Maxima and minima values of MEP are represented by black and cyan dots, respectively.

Homodimers

A total of 22 different structures have been identified corresponding to homodimer complexes (Figure 2). They have been sorted according to the type of interaction involved and different configurations. In complex **1** halogen···halogen type I interactions[77, 78] were found between both X atoms of both molecules. Complex **2** arises from pnictogen bond formation between halogen atom (donor) of one monomer and nitrogen atom (acceptor) of the other. In the case of fluorine, both monomers present approximately parallel disposition between their F-N molecular axes (dihedral F-N-N-F = 158º), while the rest are slightly distorted with dihedral X-N-N-X angles of 125.7º, 121.7º, and 118.0º for chlorine, bromide and iodine derivatives respectively. Complex **3** was only found for Cl, Br and I and involved pnictogen interactions between X atoms and π-hole, O atom and π-hole, and chalcogen-chalcogen interactions between oxygen atoms. In complex **4**, pure halogen bonds occur, but in this case, the oxygen atom acts as electron donor, instead of a halogen atom. As happened in complex **3**, complex **4** was not found for fluorine derivative. Complex **5** corresponds to an interaction between both monomers in which both molecular planes (those which contain each molecule) are perpendicular. From this configuration arise different type of interactions, pnictogen X···N and chalcogen O···O common for fluorine and chlorine derivatives, while bromine and iodine complexes are unable to establish such connections and derivate into single halogen bonds.

The measure of the X···X-N angle in those complexes informs about the final disposition. Fluorine and chlorine dimers show X-X-N angles of 136.9 and 119.71º, while bromine and iodine ones are close to 180º (164.6 and 172.2 1 respectively). Finally, complex **6** corresponds to those structures in which pnictogen (O···N) and chalcogen (O···O) interactions are found simultaneously. For these complexes, it is worth noting that fluorine derivative corresponds to a minimum in the potential energy surface, while in chlorine, bromine and iodine complexes one small negative frequency has been found (–8, –10 and –14 cm^{-1}, respectively). Those frequencies are associated to low vibrational modes, and every attempt to remove it led to complex **2**.

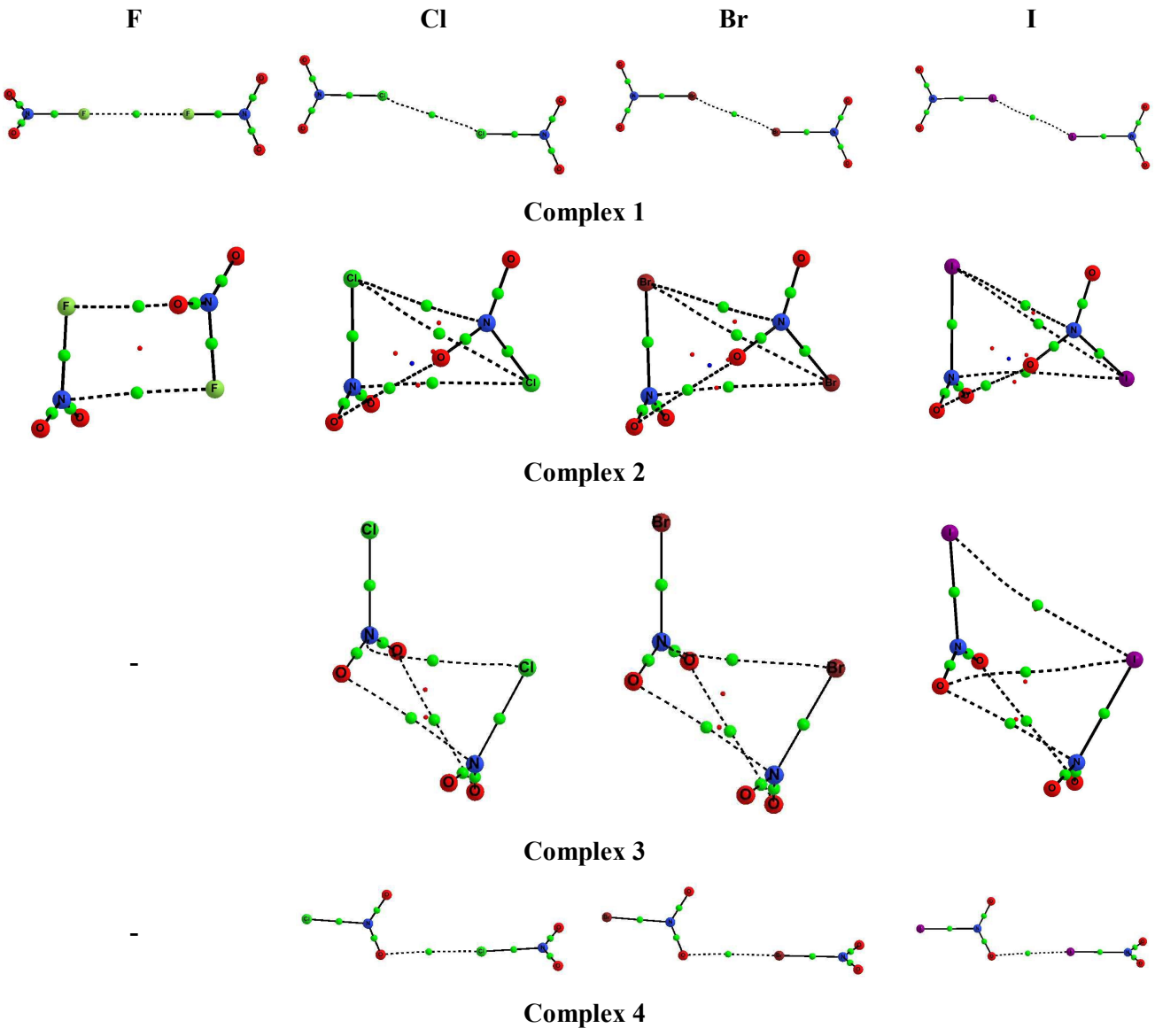

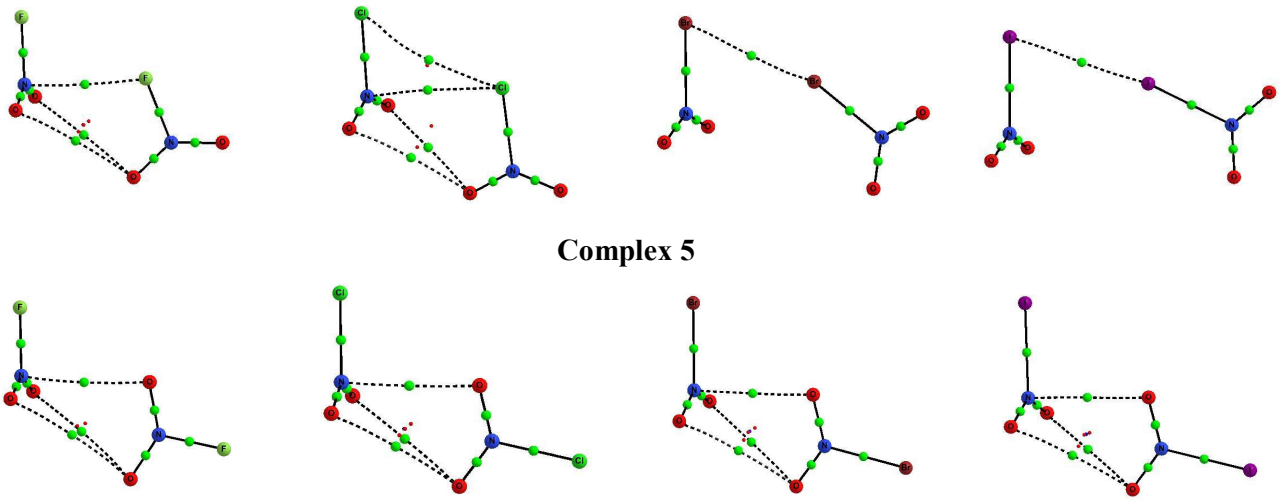

Complex 5

Complex 6

Figure 2. Molecular graphs of all compounds studied at MP2/aug-cc-pVTZ computational level. Green and red dots correspond to bond critical and ring critical points respectively.

In order to analyze the interaction energies, two different methods have been selected, MP2 and CCSD(T) both with the aug-cc-pVTZ basis set. Furthermore, the performance of the BSSE correction in intermolecular interactions has been explored as well. The basis set superposition effect (BSSE) is a simple concept, and its validity is almost universally accepted. However, recent studies suggest that for highly correlated methods such as MP2 and CCSD(T) with larger basis set, especially aug-cc-pVNZ (N=T,Q,5) ones, the validity of the counterpoise method used to evaluate the BSSE correction was questioned,[79-81] and concluded that *"that the counterpoise procedure is not justified with the use of the standard atom centered basis sets of quantum chemistry, since the basis set error (BSSE: difference of the energy with basis set limit value) will be larger for the dimer than for the atoms."* [80]

We have explored the interaction energies from MP2 and CCSD(T), both with and without the BSSE correction obtained at their corresponding computational levels (Table S1). Firstly, it is observed that BSSE values does not vary significantly across the MP2 or CCSD(T) methods. This was expected since it depends on the geometry of the complex and both values are obtained over the MP2 optimized geometry.

The inclusion of the BSSE correction decreases dramatically the interaction energy compared with uncorrected ones. This is particularly relevant in "strong" interacting complexes such as complex **1** or **4** in which a strong halogen bond occurs, and more acute with the size of the halogen considered. More disturbing is the fact that the corrected E_b, both at MP2 and CCSD(T) levels, present oscillations in their values across the halogen series, as occurs in **1**, **2** and **5,** and do not experiment the gradual decrease associated with the electronegativity of the substituent

observed previously.[82] However, if the uncorrected E_b are considered, CCSD(T) values provides accurate interaction energies with no oscillations, as one should expected for this computational level. In addition, interaction energies obtained at the basis set limit, CCSD(T)/CBS reveal similar values to those obtained at the CCSD(T)/aug-cc-pVTZ level, with slight variations for iodine derivatives.

In Table 2 the uncorrected interaction energies (E_b) at two different computational levels for all the complexes have been gathered. MP2 results tends to overestimate binding energies in comparison with the CCSD(T) results, with the exception of complex **4.** However, both methods provide similar trends, as so do CCSDT/CBS results. Considering all the compounds, E_b ranges between –1.26 to –23.41 kJ·mol^{-1} according to MP2 results, CCSD(T) shows a narrower range of –3.26 to –17.74 kJ·mol^{-1}, and CCSD(T)/CBS –2.81 to –19.27 kJ·mol^{-1}. Considering CCSD(T)/CBS interaction energies, the complex with the weakest interaction energy corresponds to complex **1**, in which a halogen bond is found, involving both halogen atoms, one from each monomer, acting as a donor and acceptor simultaneously. On the other hand, the most strongly bound complex is that with iodine, complex **4**, in which a halogen bond with oxygen acting as donor is found.

Focusing our attention to the specific energetic features within compounds belonging to the same family, MP2 results show that interaction energies evolve with the nature of the halogen considered, i.e. the interaction energy decreases with the electronegativity of X, except in complexes **2** in which an oscillation of the values is found. CCSD(T) results yields a picture similar to MP2, with an increase on the $E_b$with the size of the halogen atom in all the cases.

Linear and polynomial correlations have been found between interaction energies and the values of the MEP on the vdW (Figure S1 in Supporting Information).

Table 2. Interaction energies in kJ·mol^{-1} at MP2 [E_b(MP2)], CCSD(T)/aug-cc-pVTZ [E_b(CC)] and CCSD(T)/CBS [E_b(CBS)] computational level.

System	Sym	E_b (MP2)	E_b (CC)	E_b (CBS)	System	Sym	E_b (MP2)	E_b (CC)	E_b (CBS)
Complex **1**					Complex **4**				
F	D_{2d}	–1.26	–3.26	–2.80	F	–	–	–	–
Cl	C_2	–7.26	–3.36	–3.08	Cl	C_s	–5.46	–7.01	–7.12
Br	C_{2h}	–12.77	–5.83	–6.10	Br	C_s	–9.05	–11.25	–11.76
I	C_{2h}	–20.88	–11.15	–14.16	I	C_s	–16.15	–17.74	–19.27
Complex **2**					Complex **5**				
F	C_i	–21.84	–9.49	–7.63	F	C_s	–12.40	–10.45	–9.97
Cl	C_1	–17.09	–10.64	–9.69	Cl	C_s	–15.09	–10.73	–10.18
Br	C_1	–21.04	–15.32	–15.55	Br	C_s	–17.29	–11.28	–11.60
I	C_i	–20.77	–15.89	–15.33	I	C_s	–23.41	–15.40	–17.50
Complex **3**					Complex **6**				
F	–	–	–	–	F	C_1	–8.16	–9.65	–9.48
Cl	C_1	–15.82	–11.31	–10.47	Cl	C_s	–12.38	–11.44	–11.04
Br	C_1	–20.46	–14.73	–14.70	Br	C_s	–15.45	–13.77	–13.85
I	C_1	–21.59	–15.07	–14.91	I	C_s	–16.48	–14.33	–14.02

Atoms in Molecules theory has been used to evaluate the bonding characteristics found within complexes. Table 3 gathers the interatomic distances, electron density (ρ) at the bond critical point (BCP) and the Laplacian at the BCPs. The BCPs for all non-covalent interactions present small values of the electron density and positive Laplacian, indicating the closed shell characteristics of the weak interactions established between both moieties. Complex **1** shows a single halogen bond interaction, with electron density at BCP increasing with the size of the halogen atom considered. Complexes **2** present three different interactions according to AIM results. The first one, a X···N interaction, corresponding to the pnictogen interaction in which the halogen acts as a electron donor. The second is associated with an X···X interaction between halogens of each moiety. Finally, an O···O chalcogen interaction appears upon complexation in configuration **2**. It is noteworthy that both interactions (X···X and O···O) are not found in fluorine derivatives. Similar type of interactions to those found in complex **2**, have been found in complexes **3**. The existence of pnictogen (X···N) and chalcogen (O···O) interactions is confirmed by the presence of a BCP between the atoms involved. No X···X interaction has been found in complexes **3**, with the exception of $(INO_2)_2$ dimers. However, an additional pnictogen interaction is presented between the O atom (electron donor) and the N atom (electron acceptor). Values of ρ for those pnictogen interactions are slightly larger than those found in complex **2**, and so are the Laplacians. Chalcogen contacts present similar values than those previously found in **2**. Complex **4** shows a single halogen bond with O atom from one moiety donating into the X σ-hole of another. As occurs in complex **1**, the density properties at the BCP vary with the nature of the halogen considered,

increasing with the size of X. Type **5** complexes present two different structures: FNO_2 and $ClNO_2$ which show pnictogen X···N in addition to a bifurcated chalcogen interactions (the chlorine derivative also presents a halogen···halogen interaction), and $BrNO_2$ and INO_2 which, due to their steric impediment adopt a slightly rotated conformation respect to the formers, allowing only a halogen···halogen bond to be present. Finally, two different contacts have been found in complex **6**, pnictogen O···N and chalcogen O···O ones. Electron density values at BCP and Laplacians in O···N remain almost constant, while in chalcogen interactions both values increases with the size of the halogen atom considered.

Table 3. Interatomic distance (Å), electron density (ρ), Laplacian ($\nabla^2\rho$) (a.u.) at the bond critical point, at MP2/aug-cc-pVTZ computational level.

	Dist.	ρ	$\nabla^2\rho$	Dist.	ρ	$\nabla^2\rho$	Dist.	ρ	$\nabla^2\rho$
Complex **1**				X···X					
F	–	–	–	2.805	0.0054	0.0293	–	–	–
Cl	–	–	–	3.210	0.0102	0.0386	–	–	–
Br	–	–	–	3.204	0.0162	0.0446	–	–	–
I	–	–	–	3.313	0.0221	0.0418	–	–	–
Complex **2**	X···N			X···X			O···O		
F	2.705	0.0107	0.0546	–	–	–	–	–	–
Cl	3.273	0.0068	0.0289	3.679	0.0064	0.0221	3.040	0.0059	0.0241
Br	3.397	0.0068	0.0266	3.858	0.0068	0.0207	3.020	0.0062	0.0252
I	3.631	0.0061	0.0206	4.168	0.0066	0.0158	3.048	0.0059	0.0234
Complex **3**	X···N			O···N			O···O		
F	–	–	–	–	–	–	–	–	–
Cl	3.266	0.0073	0.0299	2.901	0.0077	0.0373	3.202	0.0045	0.0181
Br	3.369	0.0074	0.0287	2.889	0.0081	0.0386	3.158	0.0049	0.0195
I	4.285[a]	0.0055[a]	0.0139[a]	2.896	0.0081	0.0381	3.125	0.0053	0.0206
Complex **4**				O···X					
F	–	–	–	–	–	–	–	–	–
Cl	–	–	–	3.074	0.0086	0.0347	–	–	–
Br	–	–	–	3.012	0.0120	0.0443	–	–	–
I	–	–	–	2.976	0.0164	0.0548	–	–	–
Complex **5**	X···N			X···X			O···O		
F	2.784	0.0087	0.0450	–	–	–	3.143	0.0050	0.0215
Cl	3.286	0.0066	0.0282	3.648	0.0061	0.0219	3.059	0.0060	0.0255
Br	–	–	–	3.374	0.0132	0.0372	–	–	–
I	–	–	–	3.463	0.0182	0.0364	–	–	–
Complex **6**				O···N			O···O		
F	–	–	–	2.904	0.0078	0.0381	3.248	0.0043	0.0180
Cl	–	–	–	2.902	0.0083	0.0388	3.158	0.0053	0.0210

Br	–	–	–	2.892	0.0086	0.0399	3.123	0.0057	0.0228
I	–	–	–	2.927	0.0083	0.0371	3.108	0.0060	0.0234

[a] These values corresponds to a I···I halogen bond.

Among the variety of interactions established within these complexes we have found exponential relationships between the Laplacian values at the BCP and the corresponding interatomic distance, $y_{O\cdots O}=3.346\cdot e^{-1.614x}$; $y_{X\cdots N}=0.727\cdot e^{-0.978x}$, $y_{X\cdots X}=1.340\cdot e^{-1.079x}$ (Fig. 3). These relationships are in agreement with previous reports showing similar tendencies with ρ and $\nabla^2\rho$. in the same and in other weak interactions.[9, 39, 52, 82-90] Unfortunately, no fair correlations between ρ and interatomic distance have been found.

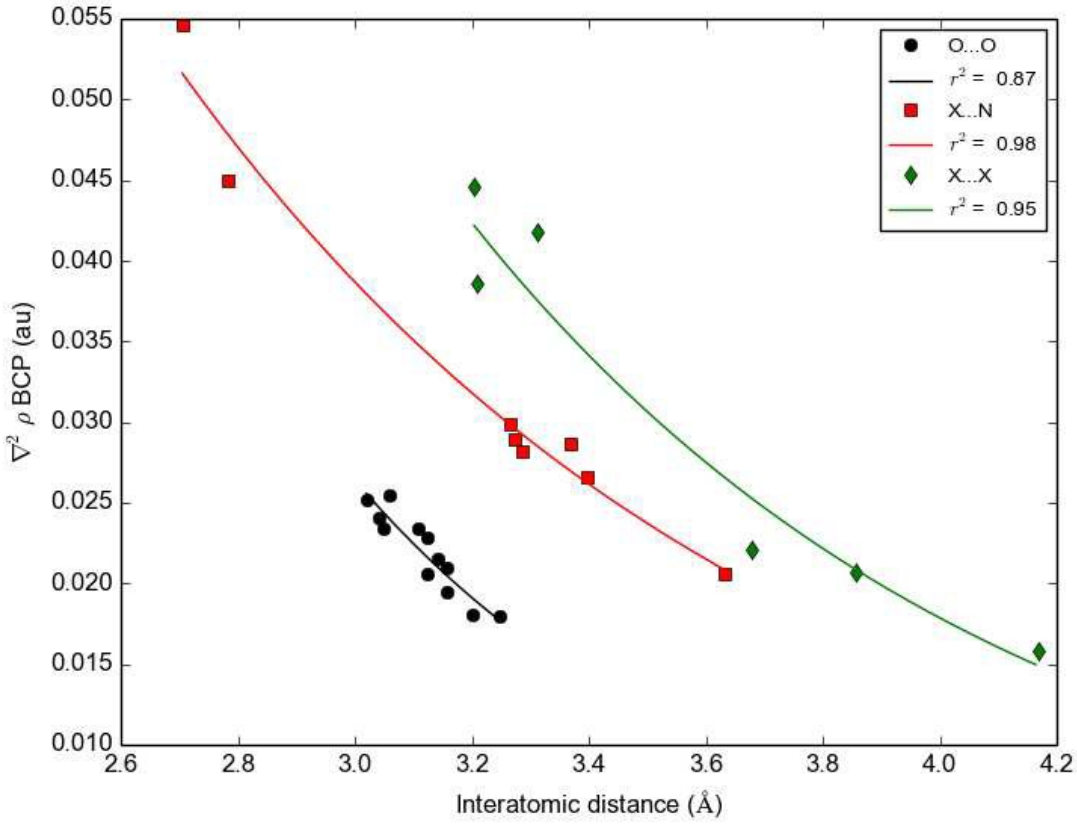

Figure 3. Exponential relationship between the value of the Laplacian at BCP (a.u.) and the interatomic distance (Å) for halogen (X···X), pnictogen (X···N) and chalcogen (O···O) interactions.

In order to achieve a visual description of the changes in the electron density upon complexation, electron density shifts (EDS) maps have been calculated and plotted in Figure 4. The yellow areas correspond to positive regions with an increase of electron density, while blue areas represent negative regions and therefore those areas with a loss of electron density upon

complexation. As observed in Figure 4 complexes **1** and **4** show relatively small positive (yellow) areas between the halogen atoms corresponding to X···X interactions. Complexes **2** show positive areas near the halogen atoms, especially in those pointing towards the nitrogen atom of the other molecules. This evidences the pnictogen interaction in which the halogen acts as donors. Complexes **3** present two main positive regions, one nearby to the halogen atom, corresponding to the pnictogen interaction (as occurs in complexes **2**) and another one belonging to the oxygen atom which acts as donor in O···O interactions. In complexes **5** and **6**, the yellow area showing an increment of the electron density upon complexation is located in the electron donor atom (halogen and oxygen respectively) towards the nitrogen atom of the other molecule. As happened in complex **2** and **3**, these EDS maps patterns are a clear indication of the pnictogen bond occurring in these complexes.

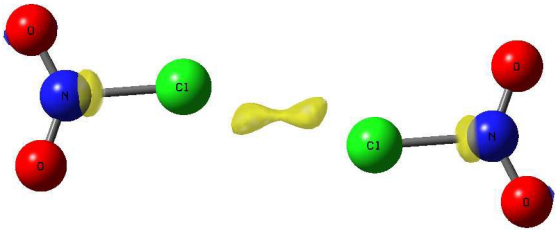

Complex **1**

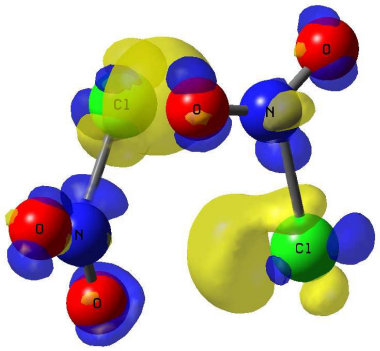

Complex **2**

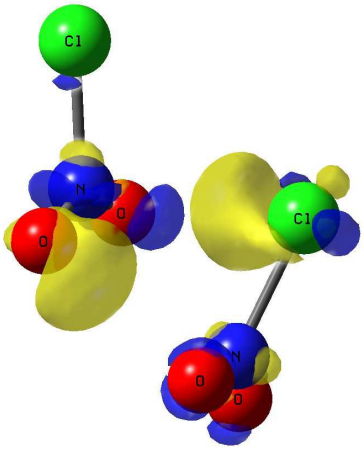

Complex **3**

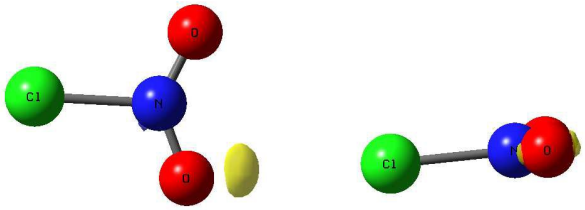

Complex **4**

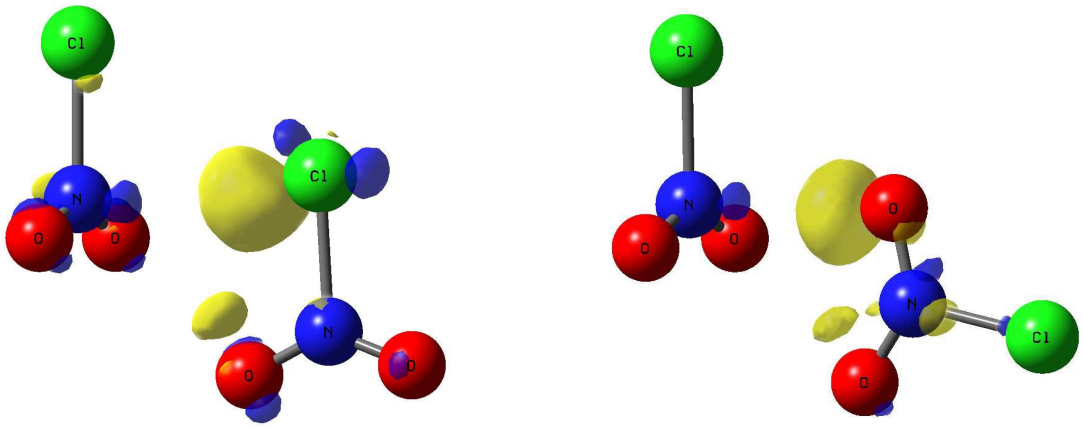

Complex **5** Complex **6**

Figure 4. Electron density shift for chlorine complexes (**1** to **6**) with an isosurface of 0.0005 a.u.

NBO analysis has been performed in order to provide an insight on the orbital interaction energies, $E^{(2)}$, in the complexes studied. NBO $E^{(2)}$ energies are presented in Table 4, in which the donation from unit 1 to unit 2 has been reported. In those cases in which both units are not identical, donation from unit 2 to unit 1 have been also taken into account. For the sake of clarity, unit 1 denotes the left hand molecule and unit 2 the right hand molecule shown in Figure 1 for each complex. Complex **1** $E^{(2)}$ energies show a donation from the X_{lp} to the σ*X-N antibonding orbital of the opposite molecule confirming the halogen bond, with an $E^{(2)}$ that increases with the atomic number of the X considered. Complex **2** present a single donation from the halogen lone pair to the π*N-O antibonding orbital, consistent with the pnictogen bond. However, while in AIM results chalcogen bonds were presents between O···O, NBO results only predict such interaction in the case of $ClNO_2$. Three different donations can be observed in complex **3**: a) donation from unit 1 O lone pairs into π*N-O (pnictogen interaction) which accounts for 3.00 kJ·mol^{-1} in all cases, b) chalcogen···chalcogen interaction, [$E^{(2)}$ between 2.2-3.3 kJ·mol^{-1}] characterised by a donation from O(1) to O(2), and c) donations from electron lone pair of halogen atom into the π*N-O (pnictogen interaction) from unit 2 to 1, varying from 1.6 to 2.0 kJ·mol^{-1}. Complex **4** present similar features than those in complex **1**, with an increasing $E^{(2)}$ with the size of the halogen, corresponding to the donation of O_{lp}→σ*X-N. In complex **5**, a wide variety of interactions are observed depending on the halogen derivative considered. FNO_2 and $ClNO_2$ show pnictogen (X_{lp}→π*N-O) and chalcogen [$O(1)_{lp}$→ O(2)lp] interactions with $E^{(2)}$ between 1.5-1.6 and 1.6-2.3 kJ·mol^{-1}l respectively. However, $BrNO_2$ and INO_2 do not only present X_{lp}→π*N-O donation (not observed with AIM theory) from unit 1 to unit 2, but also a retro donation from the halogen atom (unit 2) into the σ*X-N (unit 1). Finally, complex **6** shows O_{lp}→σ*X-N and $O(1)_{lp}$→ $O(2)_{lp}$ donations corresponding to

the pnictogen and chalcogen interactions. Those interactions present $E^{(2)}$ values between 1.5-2.8 and 1.6-3.4 kJ·mol^{-1} respectively, and present fair correlations with the interaction energies (Figure S2 in Supporting Information)

Table 4. Second order orbital interaction energies, $E^{(2)}$ in kJ·mol^{-1} at B3LYP/aug-cc-pVTZ computational level.

System	$E^{(2)}$			
	unit 1→2		unit 2→1	
Complex **1**	X_{lp}→σ*X-N			
F	0.4			
Cl	5.7			
Br	16.4			
I	39.1			
	unit 1→2			
Complex **2**	X_{lp}→π*N-O		$O(1)_{lp}$→ O(2)lp	
F	3.0			
Cl	1.6		2.5	
Br	1.8			
I	1.8			
	unit 1→2		unit 2→1	
Complex **3**	O_{lp}→π*N-O	$O(1)_{lp}$→ $O(2)_{lp}$	X_{lp}→π*N-O	
F	–	–	–	
Cl	3.0	2.2	1.6	
Br	3.0	2.3	2.0	
I	2.9	3.3	1.9	
	unit 1→2			
Complex **4**	O_{lp}→σ*X-N			
F	–	–		
Cl	7.4			
Br	15.9			
I	29.3			
	unit 1→2		unit 2→1	
Complex **5**	X_{lp}→π*N-O	$O(1)_{lp}$→ $O(2)_{lp}$	X_{lp}→σ*X-N	$O(2)_{lp}$→ $O(1)_{lp}$
F	1.6	2.3		
Cl	1.5	1.6	0.9	1.9
Br	1.9		21.4	
I	1.8		55.2	
	unit 1→2		unit 2→1	
Complex **6**	$O(1)_{lp}$→π*N-O(2)	$O(1)_{lp}$→ $O(2)_{lp}$		
F	1.5	2.3		
Cl	2.3	1.6		
Br	2.8	1.7		

I	2.6	3.4

The changes in the atomic charges in each atom (net atomic charges) upon complexation and the total charge transfer have been evaluated by means of AIM and NBO methodologies. Total charges [Q(X)] belonging to each atom and charge differences [ΔQ(X)] including charge transfer (QT) have been gathered in the supporting information (Table S1 and S2 respectively). Complexes **1** and **2**, which exhibit symmetrical interaction between both monomers, do not present charge transfer between them. However, halogen atoms show an increase in their net charge with the size of X in complex **1**, while the opposite is true for complex **2**. In complex **3**, charge transfer from unit 1 to unit 2 occurs (0.0022-0.0023 e) which is coherent with the NBO $E^{(2)}$ orbital interaction energies. Charge transferred in complex **4** varies with the electronegativity of the halogen atom considered, up to 0.03e, being more pronounced in INO_2 dimers. Complex **5** presents two different transfers depending on the interaction involved: FNO_2 and $ClNO_2$ dimers have small charge transfer between monomers upon complexation (up to 0.0019 e in chlorine derivative), but in the case of $BrNO_2$ and INO_2 the charge transfer observed is much larger than the previous F and Cl derivatives.. This is in agreement with the type of interaction found and the AIM and NBO results. Finally, complex **6** shows a charger transfer ranging from 0.001 to 0.003e. Despite the amount of charge is smaller than in the halogen bonded complexes, its variation is similar F < Cl < Br <I.

Finally, in order to evaluate the different terms of the interaction energy, SAPT-DFT calculations have been carried out. The SAPT-DFT energy terms (Tables 5 and S5) show that the dominant contributing factor to the total attractive forces is $E_D^{(2)}$, in almost all cases [with the exception of complex **2** with fluorine and complex **4** with iodine in which the electrostatic term, $E_{ele}^{(1)}$, accounts for 51% and 44%], closely followed by the dispersion one (42.1%). $E_D^{(2)}$ accounts for up to 71% of the total attractive forces, and exceptionally in complex **1** (F) it reaches up to 97.7%. The $E_{ele}^{(1)}$ is the second most important attractive term, accounting for the 51-23% of the total attractive terms. $E_i^{(2)}$ is the least important term with only 10 % of contribution. However, in complex **1** and **5**(I), $E_i^{(2)}$ overcomes the two other attractive terms, being 49.5% of the total contribution. The exchange term, $E_{ex}^{(1)}$, in all the complexes compensates the dispersion one, with the former larger than the latter. The $E_i^{(2)}$ remains almost constant along the series, not being specifically sensitive to the halogen atom considered with the mentioned exceptions (complex **1** and **5** for iodine derivatives).

In complexes **1**, the contribution of $E_D^{(2)}$ to the total attractive forces decreases with the size of the halogen considered, while the opposite is true for $E_{ele}^{(1)}$ and $E_i^{(2)}$. Similar contribution trends have been also found in complexes **3**, **4**, **5** and **6**, in which the main contributor to the attractive forces, dispersion term, decreases with the size of X, and simultaneously, the other two attractive

terms, electrostatic and induction increase. The fact that the dispersion term is dominant in halogen bonds has been previously described in the literature.[91-93] However in complexes **6**, induction term does not suffer an increase in its contribution, but a slightly decrease, in favor to the electrostatic one. Finally complexes **2** show that while $E_D^{(2)}$ increases its contribution from 42% to 60% , from fluorine to iodine derivatives, $E_{ele}^{(1)}$ decreases drastically from 50% to 29% (from F to I).

These results are consistent with the NBO ones showing that those complexes with long range interactions, which are mainly described by dispersion terms, correspond to small orbital-orbital interactions. However those particular complexes involving halogen bonds show large NBO $E^{(2)}$ interaction energies, which in SAPT results show that the dominant term of the attractive forces corresponds to the electrostatic term.

Table 5. DFT-SAPT decomposition energy at PBE0/aug-cc-pVTZ/aug-cc-pVTZ-PP for all the complexes.

System	$E^{(1)}_{el}$	$E^{(1)}_{ex}$	$E^{(2)}_{i}$	$E^{(2)}_{D}$	δHF	$\Delta E^{DFT\text{-}SAPT}$
Complex **1**						
F	0.1	3.1	–0.1	–3.6	–0.3	–0.8
Cl	–4.1	14.6	–1.0	–9.9	–2.1	–2.6
Br	–11.9	36.6	–4.2	–16.4	–5.8	–1.7
I	–26.4	56.9	–51.1	–25.6	25.6	–20.7
Complex **2**						
F	–21.2	28.0	–2.9	–17.6	–0.8	–14.7
Cl	–11.2	27.4	–1.4	–21.5	–0.9	–7.7
Br	–13.7	35.5	–1.4	–24.6	–1.1	–5.3
I	–12.6	33.0	–4.7	–25.9	1.9	–8.3
Complex **3**						
F	–	–	–	–	–	–
Cl	–8.2	23.4	–1.4	–19.6	–0.8	–6.6
Br	–11.1	31.5	–1.5	–23.0	–1.0	–5.1
I	–11.1	31.2	–4.1	–25.0	1.5	–7.4
Complex **4**						
F	–	–	–	–	–	–
Cl	–5.3	11.8	–0.5	–9.2	–1.3	–4.4
Br						
I	–23.5	36.1	–11.9	–18.4	1.7	–15.9
Complex **5**						
F	–8.8	15.1	–0.9	–12.6	–0.5	–7.6
Cl	–9.5	21.9	–0.8	–17.8	–0.9	–7.1
Br	–17.0	39.2	–3.0	–19.9	–3.9	–4.6
I	–29.0	53.3	–38.5	–26.9	20.7	–20.6
Complex **6**						

F	–3.8	12.1	–0.9	–11.6	–0.3	–4.5
Cl	–7.8	18.3	–0.7	–15.3	–0.8	–6.4
Br	–10.4	23.9	–0.7	–17.4	–1.1	–5.6
I	–11.3	24.7	–1.1	–18.6	–1.0	–7.3

Conclusions

A theoretical study of the interaction between XNO_2 monomers (X = F, Cl, Br and I) has been carried out by means of MP2 and CCSD(T) methodologies. A total of 22 different homodimers (see Figure 2) have been found upon complexation. Those structures have been sorted into six different families of complexes, according to the nature and type of interaction within each complex.

Complexes **1** and **4** present single halogen-halogen bonds while complexes **2** and **3** show pnictogen interactions in addition to O···O interactions. In complexes **5** a different variety of interactions have been found, including pnictogen (X···N), halogen (X···X) and O···O interactions. Finally, complexes **6** present pnictogen interaction with O atoms as donors, and O···O contacts.

Interaction energies are in the range of non covalent interactions, between –1.26 to –23.41 $kJ \cdot mol^{-1}$ with respect to the MP2/aug-cc-pVTZ method. CCSD(T) results present a slightly narrower range than MP2 of –3.26 to –17.74 $kJ \cdot mol^{-1}$. Those ranges of energies confirm the weak nature of the interaction found.

Benchmark calculations have been carried out confirming that in this particular study, uncorrected CCSD(T) method provides more reliable interaction energies than BSSE corrected ones, consistent with which was found for another type of interactions in the literature. The influence of the different interactions is reflected in the interaction energy of each compound. Those complexes with larger number of interactions (complexes **2**, **3**, **5** and **6**) present more negative interaction energies than those with a single halogen bond, with the only exception of complex **4** for iodine. In other words, the combination of pnicogen, chalcogen and halogen bonds results into stronger bonded complexes.

The characteristics of each interaction in the different types of complexes analysed by means of AIM reveals different type of interactions. In those complexes with only halogen bonds (complexes **1** and **4**), Laplacian and electron density at the bond critical points varies with the size of halogen atom considered, but this is not observed in the rest of the complexes. Moreover, exponential relationships have been found between Laplacian values and interatomic distances for each type of interaction: halogen (R^2 = 0.95), pnictogen (R^2 = 0.98) and chalcogen (R^2 = 0.87), which confirms the nature of the interactions found as non covalent ones.

The NBO analysis showed that halogen bonds present the largest $E^{(2)}$ orbital interaction energies, ranging from 5.7 to 39.1 kJ·mol^{-1}. Small donations from O_{lp} and X_{lp} into the π*N-O antibonding orbital characterise pnictogen bonds with values up to 3.0 kJ·mol^{-1}. Chalcogen interactions exhibit $E^{(2)}$ values similar to those in pnictogen interactions. Charge transfer between monomers indicates that complexes 5 present the largest charge transfer amongst all the complexes studied. Complexes with only halogen bonds (**1** and **4**) show larger values of $E^{(2)}$ than those with multiple simultaneous interactions (**2**, **3**, **5**, and **6**) though the interaction energies indicate that the latter are stronger bonded .

Finally, SAPT-DFT has been used to evaluate the different terms of the interaction energy finding that the most important attractive term in most cases corresponds to the dispersion, followed by the electrostatic one. Induction term remains almost constant, with the exception of complex **1** and **5** for iodine derivative in which and $E_i^{(2)}$ shows the maxima contribution to the total forces.

Acknowledgments

We gratefully acknowledge support from the Ministerio de Economía y Competitividad (Project No. CTQ2012-35513-C02-02) and the Comunidad Autónoma de Madrid (Project FOTOCARBON, ref S2013/MIT-2841). G.S.–S. wants to thank Human Frontier Science Program (Project Reference: LT001022/2013-C) for the support. Generous allocation of computing time at the TCHPC (TCD, Ireland), Irish Centre for High-End Computing (ICHEC), CTI(CSIC) and Centro de Computación Científica of the Universidad Autónoma de Madrid for the provision of computational facilities and support. Aoife Crowe is acknowledged for her careful reading and help.

References

1. K. Müller-Dethlefs and P. Hobza, *Chem. Rev.*, 2000, **100**, 143-168.
2. E. Arunan, G. R. Desiraju, R. A. Klein, J. Sadlej, S. Scheiner, I. Alkorta, D. C. Clary, R. H. Crabtree, J. J. Dannenberg, P. Hobza, H. G. Kjaergaard, A. C. Legon, M. B. and D. J. Nesbitt, *Pure Appl. Chem.*, 2011, **83**, 1637-1641.
3. P. Metrangolo and G. Resnati, eds., *Halogen Bonding: Fundamentals and Applications*, Springer, Berlin, 2008.
4. I. Rozas, I. Alkorta and J. Elguero, *Chem. Phys. Lett.*, 1997, **275**, 423-428.
5. I. Alkorta, I. Rozas and J. Elguero, *J. Phys. Chem. A*, 2001, **105**, 743-749.
6. A. Bauzá, T. J. Mooibroek and A. Frontera, *Angew. Chem. Int. Ed.*, 2013, **52**, 12317-12321.
7. S. J. Grabowski, *Phys. Chem. Chem. Phys.*, 2014, **16**, 1824-1834.
8. G. Sánchez-Sanz, C. Trujillo, I. Alkorta and J. Elguero, *ChemPhysChem*, 2012, **13**, 496-503.
9. G. Sánchez-Sanz, I. Alkorta and J. Elguero, *Mol. Phys.*, 2011, **109**, 2543-2552.
10. L. Azofra, I. Alkorta and S. Scheiner, *Theor. Chem. Acc.*, 2014, **133**, 1-8.

11. P. Sanz, M. Yáñez and O. Mó, *Chem. Eur. J.*, 2003, **9**, 4548-4555.
12. M. Widhalm and C. Kratky, *Chem. Ber.*, 1992, **125**, 679-689.
13. R. S. Drago, N. Wong and D. C. Ferris, *J. Am. Chem. Soc.*, 1991, **113**, 1970-1977.
14. F. Carré, C. Chuit, R. J. P. Corriu, P. Monforte, N. K. Nayyar and C. Reyé, *J. Organomet. Chem.*, 1995, **499**, 147-154.
15. M. R. Sundberg, R. Uggla, C. Viñas, F. Teixidor, S. Paavola and R. Kivekäs, *Inorg. Chem. Commun.*, 2007, **10**, 713-716.
16. S. Scheiner, *J. Chem. Phys.*, 2011, **134**, 094315-094319.
17. M. Solimannejad, M. Gharabaghi and S. Scheiner, *J. Chem. Phys.*, 2011, **134**, 024312-024316.
18. S. Zahn, R. Frank, E. Hey-Hawkins and B. Kirchner, *Chem. Eur. J.*, 2011, **17**, 6034-6038.
19. S. Scheiner, *Phys. Chem. Chem. Phys.*, 2011, **13**, 13860-13872.
20. S. Scheiner, *CrystEngComm*, 2013, **15**, 3119-3124.
21. S. Scheiner and U. Adhikari, *J. Phys. Chem. A*, 2011, **115**, 11101-11110.
22. U. Adhikari and S. Scheiner, *J. Phys. Chem. A*, 2012, **116**, 3487-3497.
23. U. Adhikari and S. Scheiner, *Chem. Phys. Lett.*, 2012, **532**, 31-35.
24. S. Scheiner, *Chem. Phys. Lett.*, 2011, **514**, 32-35.
25. S. Scheiner, *J. Chem. Phys.*, 2011, **134**, 164313-164319.
26. U. Adhikari and S. Scheiner, *J. Chem. Phys.*, 2011, **135**, 184306-184310.
27. Q.-Z. Li, R. Li, X.-F. Liu, W.-Z. Li and J.-B. Cheng, *J. Phys. Chem. A*, 2012, **116**, 2547-2553.
28. Q.-Z. Li, R. Li, X.-F. Liu, W.-Z. Li and J.-B. Cheng, *ChemPhysChem*, 2012, **13**, 1205-1212.
29. A. Bauzá, D. Quiñonero, P. M. Deyà and A. Frontera, *Phys. Chem. Chem. Phys.*, 2012, **14**, 14061-14066.
30. S. Ghosh, S. Biswas, A. Bauzá, M. Barceló-Oliver, A. Frontera and A. Ghosh, *Inorg. Chem.*, 2013, **52**, 7508-7523.
31. H. Zhuo, Q. Li, W. Li and J. Cheng, *New J. Chem.*, 2015, **39**, 2067-2074.
32. I. Alkorta, G. Sánchez-Sanz, J. Elguero and J. E. Del Bene, *J. Chem. Theor. Comput.*, 2012, **8**, 2320-2327.
33. J. E. Del Bene, I. Alkorta, G. Sánchez-Sanz and J. Elguero, *Chem. Phys. Lett.*, 2011, **512**, 184-187.
34. J. E. Del Bene, I. Alkorta, G. Sánchez-Sanz and J. Elguero, *J. Phys. Chem. A*, 2012, **116**, 3056-3060.
35. J. E. Del Bene, G. Sánchez-Sanz, I. Alkorta and J. Elguero, *Chem. Phys. Lett.*, 2012, **538**, 14-18.
36. J. E. Del Bene, I. Alkorta, G. Sánchez-Sanz and J. Elguero, *J. Phys. Chem. A*, 2012, **116**, 9205-9213.
37. I. Alkorta, G. Sánchez-Sanz, J. Elguero and J. E. Del Bene, *J. Phys. Chem. A*, 2012, **117**, 183-191.
38. J. E. Del Bene, I. Alkorta, G. Sánchez-Sanz and J. Elguero, *J. Phys. Chem. A*, 2013, **117**, 3133-3141.
39. G. Sánchez-Sanz, I. Alkorta, C. Trujillo and J. Elguero, *ChemPhysChem*, 2013, **14**, 1656-1665.
40. I. Alkorta, J. Elguero and J. E. Del Bene, *J. Phys. Chem. A*, 2013, **117**, 10497-10503.
41. S. J. Grabowski, I. Alkorta and J. Elguero, *J. Phys. Chem. A*, 2013, **117**, 3243-3251.
42. J. S. Murray, P. Lane and P. Politzer, *Int. J. Quantum Chem.*, 2007, **107**, 2286-2292.
43. A. Mohajeri, A. H. Pakiari and N. Bagheri, *Chem. Phys. Lett.*, 2009, **467**, 393-397.
44. P. Politzer, J. Murray and M. Concha, *J. Mol. Model.*, 2008, **14**, 659-665.
45. J. Murray, P. Lane, T. Clark, K. Riley and P. Politzer, *J. Mol. Model.*, 2012, **18**, 541-548.
46. M. J. Molina and F. S. Rowland, *Nature*, 1974, **249**, 810-812.
47. R. P. Wayne, *Chemistry of Atmospheres*, Oxford University Press, Oxford, 1991.

48. S. Fickert, F. Helleis, J. W. Adams, G. K. Moortgat and J. N. Crowley, *J. Phys. Chem. A*, 1998, **102**, 10689-10696.
49. R. Lesclaux, F. Caralp, A. M. Dognon and D. Cariolle, *Geophys. Res. Lett.*, 1986, **13**, 933-936.
50. M. Solimannejad, V. Ramezani, C. Trujillo, I. Alkorta, G. Sánchez-Sanz and J. Elguero, *J. Phys. Chem. A*, 2012, **116**, 5199-5206.
51. M. Solimannejad, N. Nassirinia and S. Amani, *Struct. Chem.*, 2013, **24**, 651-659.
52. G. Sánchez-Sanz, C. Trujillo, M. Solimannejad, I. Alkorta and J. Elguero, *Phys. Chem. Chem. Phys.*, 2013, **15**, 14310-14318.
53. S. Roy, A. Bauza, A. Frontera, R. Banik, A. Purkayastha, M. G. B. Drew, B. M. Reddy, S. Balasubramanian, S. Das and S. K. Das, *CrystEngComm*, 2015, DOI: 10.1039/c5ce00453e.
54. T. H. Dunning, *J. Chem. Phys.*, 1989, **90**, 1007-1023.
55. D. E. Woon and T. H. Dunning, *J. Chem. Phys.*, 1995, **103**, 4572-4585.
56. K. A. Peterson, B. C. Shepler, D. Figgen and H. Stoll, *J. Phys. Chem. A*, 2006, **110**, 13877-13883.
57. J. A. Pople, M. Head-Gordon and K. Raghavachari, *J. Chem. Phys.*, 1887, **87**, 5968-5975.
58. S. F. Boys and F. Bernardi, *Mol. Phys.*, 1970, **19**, 553-566.
59. I. Alkorta, C. Trujillo, J. Elguero and M. Solimannejad, *Comput. Theor. Chem.*, 2011, **967**, 147-151.
60. A. Halkier, T. Helgaker, P. Jørgensen, W. Klopper and J. Olsen, *Chem. Phys. Lett.*, 1999, **302**, 437-446.
61. A. Halkier, W. Klopper, T. Helgaker, P. Jo/rgensen and P. R. Taylor, *J. Chem. Phys.*, 1999, **111**, 9157-9167.
62. M. J. Frisch, G. W. Trucks, H. B. Schlegel, G. E. Scuseria, M. A. Robb, J. R. Cheeseman, G. Scalmani, V. Barone, B. Mennucci, G. A. Petersson, H. Nakatsuji, M. Caricato, X. Li, H. P. Hratchian, A. F. Izmaylov, J. Bloino, G. Zheng, J. L. Sonnenberg, M. Hada, M. Ehara, K. Toyota, R. Fukuda, J. Hasegawa, M. Ishida, T. Nakajima, Y. Honda, O. Kitao, H. Nakai, T. Vreven, J. Montgomery, J. A., J. E. Peralta, F. Ogliaro, M. Bearpark, J. J. Heyd, E. Brothers, K. N. Kudin, V. N. Staroverov, R. Kobayashi, J. Normand, K. Raghavachari, A. Rendell, J. C. Burant, S. S. Iyengar, J. Tomasi, M. Cossi, N. Rega, N. J. Millam, M. Klene, J. E. Knox, J. B. Cross, V. Bakken, C. Adamo, J. Jaramillo, R. Gomperts, R. E. Stratmann, O. Yazyev, A. J. Austin, R. Cammi, C. Pomelli, J. W. Ochterski, R. L. Martin, K. Morokuma, V. G. Zakrzewski, G. A. Voth, P. Salvador, J. J. Dannenberg, S. Dapprich, A. D. Daniels, Ö. Farkas, J. B. Foresman, J. V. Ortiz, J. Cioslowski and D. J. Fox, Gaussian, Inc., Wallingford CT, 2009.
63. R. F. W. Bader, M. T. Carroll, J. R. Cheeseman and C. Chang, *J. Am. Chem. Soc.*, 1987, **109**, 7968-7979.
64. F. Bulat, A. Toro-Labbé, T. Brinck, J. Murray and P. Politzer, *J. Mol. Model.*, 2010, **16**, 1679-1691.
65. R. F. W. Bader, *Atoms in Molecules: A Quantum Theory*, Clarendon Press, Oxford, 1990.
66. P. L. A. Popelier, *Atoms In Molecules. An introduction*, Prentice Hall, Harlow, England, 2000.
67. T. A. Keith, 11.10.16 edn., 2011, pp. TK Gristmill Software,(aim.tkgristmill.com).
68. A. E. Reed, L. A. Curtiss and F. Weinhold, *Chem. Rev.*, 1988, **88**, 899-926.
69. B. Jeziorski, R. Moszynski and K. Szalewicz, *Chem. Rev.*, 1994, **94**, 1887-1930.
70. A. J. Misquitta, R. Podeszwa, B. Jeziorski and K. Szalewicz, *J. Chem. Phys.*, 2005, **123**, 214103-214114.
71. A. Hesselmann and G. Jansen, *Phys. Chem. Chem. Phys.*, 2003, **5**, 5010-5014.
72. R. Moszynski, *Mol. Phys.*, 1996, **88**, 741-758.
73. J. P. Perdew, K. Burke and M. Ernzerhof, *Phys. Rev. Lett.*, 1997, **78**, 1396-1396.
74. T. J. Lee, *Chem. Phys. Lett.*, 1993, **216**, 194-199.

75. D. C. Frost, S. T. Lee, C. A. McDowell and N. P. C. Westwood, *J. Electron. Spectrosc. Relat. Phenom.*, 1975, **7**, 331-347.
76. H.-J. Werner, P. J. Knowles, F. R. Manby, M. Sch\"utz, P. Celani, G. Knizia, T. Korona, R. Lindh, A. Mitrushenkov, G. Rauhut, T. B. Adler, R. D. Amos, A. Bernhardsson, A. Berning, D. L. Cooper, M. J. O. Deegan, A. J. Dobbyn, F. Eckert, E. Goll, C. Hampel, A. Hesselmann, G. Hetzer, T. Hrenar, G. Jansen, C. K\"oppl, Y. Liu, A. W. Lloyd, R. A. Mata, A. J. May, S. J. McNicholas, W. Meyer, M. E. Mura, A. Nicklass, P. Palmieri, K. Pfl\"uger, R. Pitzer, M. Reiher, T. Shiozaki, H. Stoll, A. J. Stone, R. Tarroni, T. Thorsteinsson, M. Wang and A. Wolf, MOLPRO, version 2010.1, a package of ab initio programs.
77. G. R. Desiraju, P. Shing Ho, L. Kloo, A. C. Legon, R. Marquardt, P. Metrangolo, P. Politzer, G. Resnati and K. Rissanen, *Pure Appl. Chem.*, 2013, **85**, 1711-1713.
78. P. Metrangolo and G. Resnati, *IUCrJ*, 2014, **1**, 5-7.
79. D. J. R. Duarte, N. M. Peruchena and I. Alkorta, *J. Phys. Chem. A*, 2015, **119**, 3746-3752.
80. Ł. M. Mentel and E. J. Baerends, *J. Chem. Theor. Comput.*, 2014, **10**, 252-267.
81. I. Alkorta, J. Elguero and S. J. Grabowski, *Phys. Chem. Chem. Phys.*, 2015, **17**, 3261-3272.
82. G. Sánchez-Sanz, C. Trujillo, I. Alkorta and J. Elguero, *Phys. Chem. Chem. Phys.*, 2012, **14**, 9880-9889.
83. O. Knop, R. J. Boyd and S. C. Choi, *J. Am. Chem. Soc.*, 1988, **110**, 7299-7301.
84. I. Alkorta, L. Barrios, I. Rozas and J. Elguero, *J. Mol. Struc. THEOCHEM*, 2000, **496**, 131-137.
85. O. Knop, K. N. Rankin and R. J. Boyd, *J. Phys. Chem. A*, 2001, **105**, 6552-6566.
86. O. Knop, K. N. Rankin and R. J. Boyd, *J. Phys. Chem. A*, 2002, **107**, 272-284.
87. E. Espinosa, I. Alkorta, J. Elguero and E. Molins, *J. Chem. Phys.*, 2002, **117**, 5529-5542.
88. I. Alkorta and J. Elguero, *Struct. Chem.*, 2004, **15**, 117-120.
89. T. H. Tang, E. Deretey, S. J. Knak Jensen and I. G. Csizmadia, *Eur. Phys. J. D.*, 2006, **37**, 217-222.
90. I. Mata, I. Alkorta, E. Molins and E. Espinosa, *Chem. Eur. J.*, 2010, **16**, 2442-2452.
91. A. J. Stone, *J. Am. Chem. Soc.*, 2013, **135**, 7005-7009.
92. S. Tsuzuki, A. Wakisaka, T. Ono and T. Sonoda, *Chem. Eur. J.*, 2012, **18**, 951-960.
93. D. J. R. Duarte, N. M. Peruchena and I. Alkorta, *J. Phys. Chem. A*, 2015, **119**, 3746-3752.